JARO 03: 332–350 (2002)
DOI: 10.1007/s101620020013

JARO
Journal of the Association for Research in Otolaryngology

CT-Derived Estimation of Cochlear Morphology and Electrode Array Position in Relation to Word Recognition in Nucleus-22 Recipients

Margaret W. Skinner,[1] Darlene R. Ketten,[2,3] Laura K. Holden,[1] Gary W. Harding,[1] Peter G. Smith,[1] George A. Gates,[4] J. Gail Neely,[1] G. Robert Kletzker,[1] Barry Brunsden,[5] and Barbara Blocker[5]

[1]*Department of Otolaryngology–Head and Neck Surgery, Washington University School of Medicine, St. Louis, MO 63110, USA*

[2]*Department of Otology and Laryngology, Harvard Medical School, Boston, MA 02114, USA*

[3]*Biology Department, Woods Hole Oceanographic Institution, Woods Hole, MA 02548, USA*

[4]*Virginia Merrill Bloedel Hearing Research Center, University of Washington, Seattle, WA 98195, USA*

[5]*Department of Radiology, Washington University School of Medicine, St. Louis, MO 63110, USA*

Received: 2 April 2001; Accepted: 10 December 2001; Online publication: 27 February 2002

ABSTRACT

This study extended the findings of Ketten et al. [Ann. Otol. Rhinol. Laryngol. Suppl. 175:1–16 (1998)] by estimating the three-dimensional (3D) cochlear lengths, electrode array intracochlear insertion depths, and characteristic frequency ranges for 13 more Nucleus-22 implant recipients based on *in vivo* computed tomography (CT) scans. Array insertion depths were correlated with NU-6 word scores (obtained one year after SPEAK strategy use) by these patients and the 13 who used the SPEAK strategy from the Ketten et al. study. For these 26 patients, the range of cochlear lengths was 29.1–37.4 mm. Array insertion depth range was 11.9–25.9 mm, and array insertion depth estimated from the surgeon's report was 1.14 mm longer than CT-based estimates. Given the assumption that the human hearing range is fixed (20–20,000 Hz) regardless of cochlear length, characteristic frequencies at the most apical electrode (estimated with Greenwood's equation [Greenwood DD (1990) A cochlcar frequency – position function of several species – 29 years later. J Acoust. Soc. Am. 33: 1344–1356] and a patient-specific constant a_s) ranged from 308 to 3674 Hz. Patients' NU-6 word scores were significantly correlated with insertion depth as a percentage of total cochlear length ($R = 0.452$; $r^2 = 0.204$; $p = 0.020$), suggesting that part of the variability in word recognition across implant recipients can be accounted for by the position of the electrode array in the cochlea. However, NU-6 scores ranged from 4% to 81% correct for patients with array insertion depths between 4% and 68% of total cochlear length. Lower scores appeared related to low spiral ganglion cell survival (e.g., lues), aberrant current paths that produced facial nerve stimulation by apical electrodes (i.e., otosclerosis), central auditory processing difficulty, below-average verbal abilities, and early Alzheimer's disease. Higher scores appeared related to patients' high-average to above-average verbal abilities. Because most patients' scores increased with SPEAK use, it is hypothesized that they accommodated to the shift in frequency of incoming sound to a higher pitch percept with the implant than would normally be perceived acoustically.

Keywords: cochlear length, cochlear implant, electrode array, computed tomography (CT), two- and three-dimensional reconstruction, word recognition

Correspondence to: Margaret W. Skinner, Ph.D. • Department of Otolaryngology–Head and Neck Surgery • Washington University School of Medicine • 660 South Euclid Avenue, Campus Box 8115 • St. Louis, MO 63110. Telephone: (314)362-7125; fax: (314)362-7522; email: skinnerm@msnotes.wustl.edu

INTRODUCTION

Multielectrode, intracochlear implants used with recent speech processors and speech-coding strategies provide more benefit than was dreamt possible when they were first introduced in the early 1980s (Helms et al. 1997; Osberger and Fisher 1999; Skinner et al. 2002). Despite this success, there is potential for increasing clinical benefits of cochlear implants by developing more effective ways to stimulate an individual's residual auditory neurons. To accomplish this goal, it is of key importance to understand the relation, among the following factors: the position of individual electrodes in a patient's cochlea; behavioral measures of threshold, growth of loudness, and pitch perception for each electrode; the evoked response of auditory neurons to electrical stimulation of the associated electrodes; and the ability of each patient to understand speech based on how his or her speech processor is programmed.

There is substantial evidence that the longitudinal position of electrodes in the cochlea correlates with the measures listed in the Precedding paragraph. For example, eight Nucleus-22 (Cochlear Corp., Englewood, CO) recipients showed a general progression of high-to-low pitch estimates for electrodes of increasing insertion depth based on each electrode's angular position determined from two-dimensional (2D) radiographs (Cohen et al. 1996a). For 20 recipients of the same device, there was a significant linear correlation ($R = 0.59$, $p < 0.006$) between CID sentence scores and insertion depth of the most apical electrode determined from 2D radiographs (Marsh et al. 1993). For three recipients of the Nucleus-22 who used 4-electrode SPEAK programs, vowel and consonant recognition decreased as the location and spacing of activated electrodes departed from the normal acoustic tonotopic pattern or from that learned experience with through 20-electrode programs (Fu and Shannon 1999a). This tonotopic pattern was based on the surgeon's report of the depth of insertion as described below.

Adult cochlear implant recipients who became deaf after learning language vary widely in their ability to recognize words and sentences presented at 70 dB SPL without visual cues. Blamey et al. (1996) have suggested a model of auditory performance and a model of ganglion cell survival in this population to describe primary and secondary factors that affect these patients' scores. Primary factors include group factors (e.g., the implant system; speech materials and evaluation environment; and the surgical, audiological, and rehabilitative procedures used) and individual factors (e.g., number of electrodes and their position in the cochlea; electrical properties, size, and physical condition of the cochlea; spiral ganglion cell survival and function; central neural function, memory for spoken language, and cognitive function). The relation between these primary factors and secondary factors (e.g., etiology, age, duration of deafness, and duration of implant use) also are described. Analysis of data from 808 implant recipients from published and unpublished sources showed a strong negative effect of duration of deafness, a slight negative effect of age at implantation after 60 years of age, and a positive effect of duration of implant use on auditory performance. This last result suggests that there is a learning and/or neural plasticity effect that enables adult recipients to recognize speech better given experience using their devices in everyday life. When effects of duration and age at onset of deafness were subtracted, etiology was shown to have a statistically significant effect. Those with bacterial labyrinthitis performed significantly below the rest of the group. It is clear that many factors interact in complex ways to affect individual recipients' scores on auditory speech tests (e.g., open-set word and sentence tests presented in quiet or in noise). As one factor contributing to the variability in implant recipients' ability to understand speech spoken without visual cues, further study of the relation between the position of the electrode array in the cochlea and word recognition is warranted.

To date, four approaches for estimating the *in vivo* intracochlear position of implanted electrode arrays have been reported. The first is calculated from the surgeon's report of how much of the array was inserted into the inner ear, the manufacturer's specifications of electrode spacing, and the average length of human cochleae. Using this approach, Fu and Shannon (1999a,b,c) estimated the longitudinal position of each implanted electrode and the associated characteristic frequencies of nearby neurons using Greenwood's formula (Greenwood 1990) based on an average cochlear length (35 mm) and a frequency range of 20–20,000 Hz.

The second approach is based on analysis of 2D radiographs according to a technique developed by Marsh et al. (1993) and extended by Cohen et al. (1996b) and Xu et al. (2000). This technique utilizes a digitized 2D radiograph of the patient's implanted temporal bone that shows each band (i.e., electrode and supporting bands), the vestibule, superior semicircular canal, and some neighboring structures (Xu et al. 2000). A reference line is drawn from the apex of the superior semicircular canal through the midpoint of the vestibule and the electrode lead wires (see Fig. 6 in Xu et al. 2000). A mathematical spiral template is fitted to the band images on the 2D radiograph such that the center point of the spiral (i.e., the cochlear or modiolar axis) and the size of the

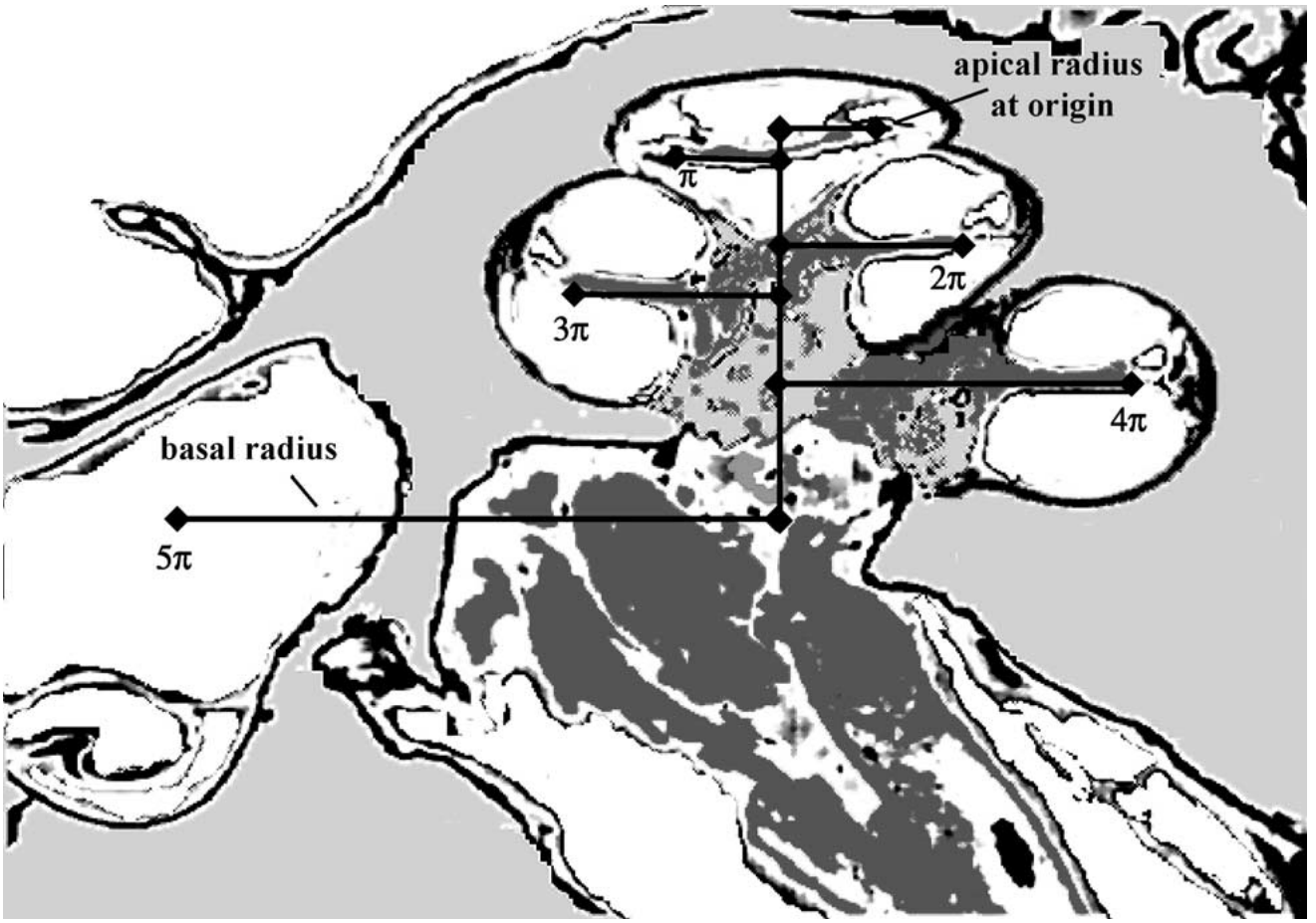

FIG. 1. Measured radii illustrated on a schematized image of a midmodiolar section of a human cochlea. Turns in radians are shown for each major radius. Axial height is represented by the vertical line drawn from the basal most radius to the apical radius at the spiral origin.

spiral template are allowed to vary to reflect variation in cochlear size. A line is drawn from the estimated center point perpendicular to the reference line. Each electrode's longitudinal position is defined in degrees rotation from 0° (i.e., the intersection of the reference line and the line through the spiral center point). Each electrode's position is plotted between outlines of the cochlear inner and outer walls, the average positions of which were estimated from analysis of human temporal bones. This method takes into account individual variations in cochlear size but not total number of cochlear turns. The estimate of the characteristic frequency (Hz) associated with each electrode's position in insertion angle (degrees) is derived from Bredberg's data (Bredberg 1968) and Greenwood's formula (Greenwood, 1990) for a human hearing range of 20–20,000 Hz (Cohen et al. 1996b).

The third approach to estimating the *in vivo* intracochlear position of implanted electrode arrays is based on analysis of high-resolution images of the implanted array and cochlea reconstructed at 100-μm slice intervals from spiral computed tomography (CT) scan data as described by Ketten et al. (1998). The basilar membrane, organ of Corti, and Reissner's membrane are not resolvable in any CT image. Therefore, calculations of each patient's 3D cochlear length from CT scans are based on measurements made of radii from the center of the fluid space of the cochlear canal to the modiolar axis (see Fig. 1; equations in Ketten et al. 1998). The depth of electrode array insertion is referred to as its distance along this 3D cochlear canal length. Electrode array insertion depth is expressed in both millimeters and percentage of cochlear canal length, and, using Greenwood's equation (Greenwood 1990), frequency distributions for both the array and total cochlear canal length are calculated for each individual. An assumption in this study was that given the large variation in human cochlear length (28–40 mm; Ulehlova et al. 1987), it is more exact to base frequency distributions on individual estimates of cochlear length rather than, have an arbitrary average distribution.

In a fourth approach, Kelsall et al. (1997) integrated information provided by two x-ray imaging techniques to approximate more closely the position of each electrode in relation to the facial nerve and the inner ear than was possible with either technique alone. Two-dimensional radiographs (modified Stenver's view) were obtained from 11 recipients of the Nucleus-22 implant. In addition, axial and coronal nonspiral CT scans were obtained, and five points along the facial nerve course were marked on high-resolution 2D images prior to 3D reconstruction. After 3D reconstruction and appropriate rotation, the 2D radiograph (after being reduced in size) was superimposed onto the 2D CT image of the implanted array with the position of the facial nerve marked to determine the distance from each electrode to the facial nerve.

The goal of the present study is to extend the findings of Ketten et al. (1998) by (1) describing CT-derived calculations of cochlear length and insertion depth of the electrode array for 13 more adults and (2) correlating insertion depth and word recognition after one year's use of the SPEAK speech-coding strategy for these adults as well as those who used the SPEAK strategy from the Ketten et al. study. For all 26 patients, insertion depth (mm) is compared with that calculated from the surgeon's report and nominal values of array dimensions prior to implantation. In addition, insertion depth (% of total cochlear length) is compared with characteristic frequency calculations for the most apical electrode based on a fixed hearing range from 20 to 20,000 Hz. It is hypothesized that the 3D functional insertion depth of the electrode array will explain part of the variability in word recognition. It also is hypothesized that patients with average and above-average verbal skills and an etiology of deafness that does not compromise the physical status of the cochlea will learn to adapt to the shift in frequency of incoming sound to a higher pitch percept with the implant than would normally be perceived acoustically.

METHOD

Patients

This study is based on data from 26 adults implanted with the Nucleus-22 electrode array who participated in a longitudinal research study for which their word recognition scores were obtained. *In vivo* measures of the cochlear length and insertion depth of the array were obtained from 13 adults in this study and combined with those for the 13 of 20 adults in the Ketten et al. study (1998) who used the SPEAK speech-coding strategy for one or more years. As shown in Table 1, these 26 patients represented a wide range of years of deafness prior to implantation, age at implantation, number of electrodes and supporting bands inserted into the cochlea, and etiologies. Patients 1 through 13 (hereafter referred to as P1, . . ., P13) are those for whom cochlear and array measurements were obtained in this study, and P14 through P26 are those for whom measurements were made by Ketten et al. (1998; P1, P2, P3, P4, P6, P9, and P14 through P20 are the same as P14 through P26 in this study). Patients were implanted by surgeons affiliated with Washington University School of Medicine. All except P13 participated in weekly postoperative programming and hearing rehabilitation services in the Cochlear Implant Program for the first three months after initial stimulation. P13 began to receive these services nine months after implantation, and evaluation of word recognition in the longitudinal study began at one year instead of three months after initial stimulation. Protocols for use of human subjects in this study were reviewed and approved by the Washington University School of Medicine Human Studies Committee.

For P1 through P13, a postoperative CT scan was obtained under a research protocol at times after implantation that ranged from 1 to 10 years; for P14 through P26, the CT scan was obtained at 0.1 year after implantation as part of their clinical care (see Table 2). Word recognition scores that were correlated with the insertion depth of the most apical electrode determined from CT scans were those obtained after using the SPEAK speech-coding strategy for one year. This arbitrary choice was based on the assumption that one year was sufficient time for most patients to acclimate to this strategy and to the shift in assignments of frequency bands of incoming sound to electrodes that were used with earlier speech-coding strategies. Because speech recognition has been shown to be successively higher with the F0F1F2 (Dowell et al. 1987), multi speak (MPEAK; Skinner et al. 1991), and spectral peak (SPEAK; Skinner et al. 1994) strategies in the same patients (Fig. 1 in Skinner 1999), it was important to compare subjects' scores obtained with the same strategy with electrode array insertion depth. As shown in Table 2, 21 of the 26 patients used MPEAK prior to using SPEAK, and 7 of these 21 patients also used F0F1F2. The years of implant use when the word score was obtained ranged from 1 to 8 (mean = 3.4 years), and the age when this score was obtained ranged from 30 to 83 years (mean age = 60.8 years). To provide an approximation of the improvement in word score from the first score that was obtained with SPEAK to the highest score during SPEAK use, the difference in percentage points is also included in Table 2. Also shown in Table 2 is the number of years of SPEAK use each patient had at the time the highest score was obtained. Note that the scores decreased for P19 and P26. P19

TABLE 1

Patient profiles

Patient	*Sex*	*Yrs of profound deafness*	*Age at implantation*	*Ear implanted*	*Bands inserted*	*History*
1	M	17	60	L	23	Otosclerosis
2	F	4	60	L	25	Lues
3	F	9	26	R	24	Meningitis
4	M	17	38	R	27	Severe head trauma
5	M	4	61	L	32	Acoustic trauma
6	F	2	52	L	32	Lues
7	M	10	61	R	32	Otosclerosis
8	F	17	45	R	32	Maternal rubella
9	F	0.25	35	R	27	Unknown
10	M	21	47	L	20	Genetic
11	M	1	43	R	29	Genetic
12	F	15	70	L	32	Unknown
13	F	1	58	R	20	Unknown
14	F	4	70	R	28	Progressive after measles or mumps
15	M	33	35	L	25	Progressive after maternal rubella
16	F	5	74	R	29	Unknown
17	F	4	52	R	28	Otosclerosis
18	M	12	76	R	22	Diabetes
19	F	2	72	R	29	Unknown
20	F	20	39	L	24	Progressive (L); Profound at birth (R)
21	F	0.75	72	R	30	Progressive
22	M	10	61	R	32	High fever (R); Unknown (L)
23	F	1	60	L	27	Bilateral radical mastoidectomy for chronic otitis media
24	M	0.5	59	R	32	Progressive after measles or mumps; noise exposure; Meniere's disease
25	F	25	75	R	29	Progressive after measles; bilateral radical mastoidectomy for chronic otitis media
26	F	3	82	R	28	Otosclerosis; noise exposure

no longer uses her implant because of advanced Alzheimer's disease, and P26 died at the end of two years. Preoperatively, 16 of the 26 patients were evaluated with the Wechsler Adult Intelligence Scale-Revised (Wechsler 1981) as part of their clinical psychological evaluations. Because patients' verbal abilities affect word recognition, their verbal IQ scores are included in Table 2.

Patients had speech processor programs that differed in electrode-pairing mode, the most apical active electrode that was included in the program, and the frequency band of incoming sound that was assigned to this electrode as shown in Table 3. Bipolar pairing modes included BP+1, BP+2, and BP+3 for which the active electrode was separated from the more apical return electrode by 1, 2, and 3 intervening electrodes, respectively. For example, the most apical electrode programmed was usually 20 with the return electrode as 22 in the BP+1 mode; for BP+2 and BP+3, the active electrodes were electrodes 19 and 18 with the return electrode as 22, the most apical electrode in any patient's array. For the Common Ground mode, all 22 electrodes can be programmed as the active electrodes; each time an electrode is stimulated, all other electrodes in the program become the return. Three patients (P10, P17, and P20) did not have the most apical electrode in their array, electrode 22, included in their programs because it caused facial nerve stimulation or an aberrant sound quality. All three of these patients

TABLE 2

Summary of pateients' implant use and word scores

Patient	Yrs implant use at time of CT scan	Yrs F0F1F use	Yrs MPEAK use	Yrs implant use after 1 yr of SPEAK use	Age (yrs) after 1 yr of SPEAK use	Verbal IQ[a]	NU-6 word after 1 yr of SPEAK use	Improvement in NU-6 word scores during speak use	Yrs SPEAK use for highest score[a]
1	10	4	3	8	68	124	34	9	3
2	10	2	4	6	68	114	28	12	7
3	7	0	2	3	30	118	81	14	2
4	8	1	3	5	43	124	70	16	2
5	9	1	3	5	67	87	56	23	3
6	10	1	4	6	58	CNT	18	7	1
7	10	1	4	6	73	136	67	8	1
8	9	0.25	4	5	50	77	52	10	2
9	7	0	3	4	38	93	58	7	6
10	7	0	4	4	51	111	7	2	3
11	2	0	0	1	44	DNT	71	27	3
12	6	0	1	2	72	DNT	53	21	3
13	1	0	0	1	59	DNT	10	17	3
14	0.1	0	3	4	74	117	63	12	5
15	0.1	0	3	4	39	73	27	19	3
16	0.1	0	4	4.5	78	83	14	NA	NA
17	0.1	0	3	3	56	114	15	11	3
18	0.1	0	3	4	80	DNT	12	7	3
19	0.1	0	2	3	75	75	34	−11	3
20	0.1	0	1	2	41	95	25	9	5
21	0.1	0	1	2	74	DNT	66	6	1
22	0.1	0	1	2	63	DNT	69	21	1
23	0.1	0	1	2	62	DNT	54	17	4
24	0.1	0	0	1	60	DNT	72	10	0.33
25	0.1	0	0	1	76	DNT	4	6	2
26	0.1	0	0	1	83	DNT	26	−4	2

[a]Abbreviations: CNT=could not test; DNT=did not test; NA=Patient died before more than one test was obtained.

used the Common Ground mode because it provided them better understanding of speech than the bipolar modes. The assignment of frequency boundaries of incoming sound to electrodes is accomplished by the use of preset tables. Most of the patients used preset Table 7 that assigned the frequency band from 120 to 280 Hz to the most apical active electrode as shown in Table 3. A few used slightly higher frequency bands (i.e., 133–311 Hz or 150–350 Hz) because the sound quality was less high-pitched and more acceptable to them for use in everyday life.

Scan procedure

All 26 patients were scanned postimplantation by a Siemens SOMATOM Plus-S or Plus-4 single-row spiral CT scanner (Siemens, Munich, Germany) using the following parameters: spiral protocol, 1-mm increment at 1-mm/s table speed, 215 mA, 120 kV. The gantry tilt of the scanner was adjusted so that the scanning line through the patient's head paralleled a line through the inferior margin of the zygomatic arch and the superior margin of the petrous bone on the topogram. The Ketten projection approximates the inverse of the conventional Stenver's projection and has been shown to provide paramodiolar sections that allow direct comparison with histologic studies (Ketten 1994; Ketten et al. 1998). A midmodiolar projection (see Fig. 1) also provides the most accurate measurements for cochlear length (Takagi and Sando 1989; Ketten 1994). In those patients for whom the original scans did not provide a paramodiolar projection, reformatted paramodiolar images were obtained from 3D reconstructions of the inner ear with Siemens software. Preoperative scans were reviewed for P12 and P14 through P26 for the Ketten et al. study (1998). They were not available for the other patients.

Image reconstruction

Images were reconstructed with an ultra-high-resolution kernel, 512 matrix, and tenfold expansion of the attenuation scale to improve discrimination of the metallic components of the electrode array. Images

TABLE 3

Speech processor program information

Patient	*Electrode pairing mode*[a]	*Most apical active electrode*	*Frequency band assigned to the most apical electrode (Hz)*
1	BP+3	18	150–350
2	BP+3	18	120–280
3	BP+1	20	120–280
4	BP+1	20	150–350
5	BP+1	20	133–311
6	BP+1	20	120–280
7	BP+3	18	120–280
8	CG	22	120–280
9	BP+2	19	150–350
10	CG	20	120–280
11	BP+1	20	120–280
12	BP+2	20	120–280
13	CG	22	120–280
14	BP+1	20	120–280
15	BP+1	20	120–280
16	BP+1	20	133–311
17	CG	18	133–311
18	BP+1	20	120–280
19	BP+1	20	120–280
20	BP+1	20	120–280
21	CG	20	120–280
22	BP+1	20	133–311
23	BP+2	19	120–280
24	BP+1	20	120–280
25	BP+1	20	120–280
26	BP+1	20	120–280

[a]Bipolar modes: BP+1, BP+2, BP+3 (see text for description); Common Ground mode: CG.

were reconstructed initially at 1-mm slice intervals through the entire scan. These ''baseline'' images were examined to determine the scanner table positions that encompassed each patient's cochlear canal and vestibular system. This subset of each patient's scans was reconstructed from the original attenuation data at 0.1-mm slice increments and a magnification of 9.8. Consequently, for each patient's implanted ear, a study series that consisted of approximately 100–150 images was reconstructed with 100-μm isotropic voxels

Measurements of an individual's cochlear radii, hook length, and position of electrode tip and entry points

Cochlear measurements were taken of the cochlear radii for each turn in each patient's midmodiolar or closest paramodiolar section, as shown in the schematized image in Figure 1. Additional quarter-turn radii were derived from images based on the table position of slices containing the superior and inferior margins (i.e., tangential sections) of the cochlea. As a check on these measures, a reformatted image showing the spiral axis or orthogonal projection was produced, and measurements taken for the radii in this projection were compared with the modiolar measures. Measurements of the length of the quarter-turn radii were taken at right angles from the modiolar axis to the centroid of the cochlear canal bony margins because the basilar membrane and cochlear scalae divisions are not imageable by current CT procedures. This point (Fig. 1) falls approximately at the juncture of the basilar membrane and osseous spiral lamina and is therefore near but slightly medial of the pillar cell mark conventionally used in histologic studies. In postimplantation images, the blooming artifact of the electrode array sometimes made it difficult to determine the exact position of the outer cochlear wall. In this case, attenuation measures were made to estimate wall position, but, of necessity, the estimation of the center of the original fluid space was less exact. The axial height of the cochlea is the modiolar axis length subtended through the modiolus from the apical to the basal radial planes (i.e., length of the vertical line in Fig. 1). The length of the hook was measured by determining its midcanal center in successive 0.1-mm slices from the beginning of the first turn to the end of the cochlear canal at the round window. The number of

cochlear turns was measured from the apical end of the cochlear canal to the beginning of the first turn. As described by Ketten et al. (1998), measurements of the radii and axial height were made from hard copies of CT images with steel calipers and repeated under 2X–7X magnification with an Olympus stereomicroscope (Olympus America, Inc., Melville, NY). Measurements were repeated until three were within 0.05 mm. The average of these three measurements was used as the final number for each cochlear canal measurement.

Calculation of an individual's cochlear canal length

Ketten's method for estimating 3D cochlear length (Ketten et al. 1998) assumes that the Archimedean spiral provides the single closest fit of any regular curve for the midline of the average human cochlear canal excluding the hook region and that the cochlear spiral has a relatively common configuration in all patients. These assumptions are based on comparisons of CT and histologic measurements of cochlear radii and length from cadaveric studies (Ketten and Wartzok 1990; Ketten et al. 1998). The conventional electrode array, however, has a slightly different path and may be best fitted by a different spiral (Nadol et al., 2001) as described below.

For each patient, the cochlear spiral constant a was calculated from the modiolar radii (Ketten and Wartzok 1990). Because there are substantial differences in apical, middle, and basal turn diameters among individuals but the spiral shape is relatively regular within each patient, the value of a gives calculated on an individual basis, although there is little variation for this constant among individuals as shown in Table 3. Cochlear canal length was calculated as the 3D spiral path length from the cochlear apex to the end of the first turn, and then the hook length was added (Table 3) as described in Ketten et al. (1998).

Calculation of the functional insertion depth of an individual's implanted electrode array from CT scans

A number of patients had kinks, bends, and compressions in their implanted arrays such that the cochlear penetration of the implanted array was often shorter than its apparent implanted length estimated by the surgeon's report of the number of rings inserted. In some cases, the array entry point was also well past the hook or the hook area was obliterated by a drillout procedure. For this reason, a functional insertion depth was calculated that corresponded to the apical position of the array rather than simple array length *per se*. The functional insertion depth is based on the apical most point of the array as well as canal and array radii as determined from the CT scans.

The location of the most apical electrode was determined by examining the appropriate sequence of images and identifying the first submillimeter slice in which the attenuation was consistent with the platinum electrode band (approximately 20,000–25,000 Hounsfield units [HU]). The angular position of this tip electrode from the apical end of the cochlear canal was marked on a schematic showing a 2D projection drawing representing the turns for each individual, plotted versus table position in mm. The entry of the electrode array into the cochlear canal was similarly plotted from reformatted submillimeter slices. Three orthogonal plane views were reformatted and compared for each cochlea to localize the cochleostomy site (see Fig. 4 in Ketten et al. 1998). Lastly, 3D reconstructions of the digitally isolated array for each patient were reviewed and compared with the 2D images to determine the intracochlear position of kinks, twists, and compressions in the array that deviated from the ideal scala–tympani-insertion path (e.g., see Fig. 2 of this article and Figs. 6, 7, and 8 in Ketten et al. 1998).

Array location, including electrode and supporting bands, the elevation within the cochlea from the tip electrode to the array entry into the lower basal turn, and approximate scalae position were similarly mapped onto the turn schematics and the angular distribution; that is, the angular rotation of the array was measured. The 3D functional insertion length was determined by calculating the arc length from the apex of the cochlea back to the most apical electrode position (i.e., the array tip) and subtracting that from the total cochlear length obtained as described above.

Calculation of insertion depth of an individual's implanted array from surgeon's observations

Implantation of these patients was performed by four surgeons who had different criteria for determining whether a stiffening band entered the cochlea. For P3, P9, P10, and P14 through 19, lengths were calculated by multiplying the number of electrodes and bands reported inserted by the surgeon (Table 1) times the manufacturer's specifications for electrode and stiffening band length (0.300 mm) plus interelectrode distance (0.450 mm). This particular surgeon's report stated that the last intracochlear band was flush with the lateral surface of bone around the cochleostomy. For all the other patients, 0.300 mm was added to each length calculation to compensate for an average 1-band-length difference that would

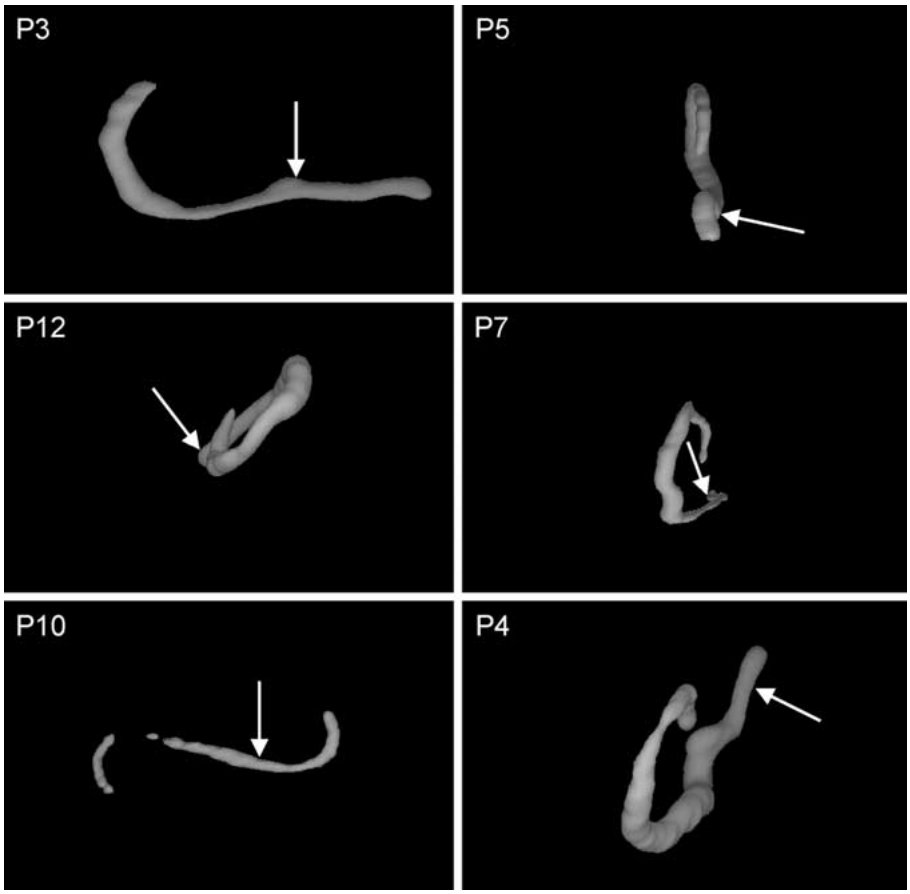

FIG. 2. 3D reconstructed images of the electrode array for P3, P12, P10, P5, P7, and P4. The arrow shows the point at which the electrode array enters the cochlea on each image. The 3D orientation of P3's array was rotated so that cochlear axis is perpendicular to the image. P12's array was rotated to show the elevation of the most apical electrode above the most basal portion of the array as well as the elevated curvature of the array as it ascends into the upper basal turn. P1O's array was rotated to show the compression of the array and most apical electrode. P5's array was rotated to show the U-shaped kink just before its entry into the cochlea with the ascending curvature in the lower basal turn. P7's array was rotated to show the right angle kink after its entry into the cochlea, a straight portion of the array, and then a complicated trajectory as it ascends from the lower into the upper basal turn of the cochlea. P4's array was rotated to show the very complicated trajectory with multiple kinks in the lower basal turn followed by ascent into the upper basal turn.

have resulted from reports of the other three surgeons who had more conservative criteria for reporting components as intracochlear. They reported that the last intracochlear band was at the medial surface of the bone around the cochleostomy.

Calculation of characteristic frequencies

In Ketten et al. (1998), the conventional Greenwood equation, $F = A(10^{ax} - k)$ (where F is frequency in Hz; x is distance along the cochlear canal in millimeters; and A, a, and k are constants; constant a is not the same as the spiral constant a in Ketten and Wartzok 1990), was used to calculate the characteristic frequency at specific locations along the cochlear canal in individual patients. The value $k = 0.88$ was chosen based on Greenwood's conclusion that it was the best fit for human hearing (Greenwood 1961, 1990; Greenwood and Joris 1996).

In the present article, two different sets of characteristic frequencies for the apical electrode location for each patient were calculated to compare how two different assumptions, which are currently unresolved in the literature, affect frequency distributions. The first assumption is that the total range of hearing (Hz) differs for each cochlea, given that each critical band covers the same linear distance along the basilar membrane. Based on this assumption, there are more critical bands for long cochleae than for short cochleae. The second assumption is that the hearing range is fixed in humans and the total range is 20–20,000 Hz despite individual differences in cochlear length. In this case, critical bands in different individuals have variable widths (see discussion in Ou et al. 2000). Although there is evidence to suggest that human detection at very low and very high frequencies is based on cochlear excitation patterns that span a frequency range that is smaller than 20–20,000

Hz (Moore et al. 1997; Buus et al. 1986; Zhou 1995), this model has not been verified. For this reason, the 20–20,000-Hz range was chosen for the fixed-range estimate so that the results could be compared with the range used in other studies that made this same assumption (e.g., Cohen et al. 1996b; Fu and Shannon 1999a,b,c).

Given the first assumption, patient-specific values of the constant A (i.e., A_s) and patient-specific values of the constant a (i.e., a_s) were calculated using 35 mm as the average human cochlear length. A_s was calculated from the human average constant (A_h) derived by Greenwood (165.4) and the ratio of the average human length (L_h) (35 mm) versus each patient's cochlear canal length (L_s): $A_s = (A_h \times L_h/L_s)^2$. The constant a_s, was calculated as follows, $a_s = 2.1/L_s$. The value 2.1 is obtained by multiplying the human average for a (0 0.06) derived by Greenwood (1961,1990; Greenwood and Joris 1996) by the average human cochlear length (35 mm). When a_s is used to calculate the characteristic frequency at the basal end of the cochlea with Greenwood's formula, then $x = L_s$; at the apical end of the cochlea, $x = 0.001$ mm. When a_s is used to calculate the characteristic frequency at the most apical electrode, then x equals L_s minus the distance in mm from the apex to the most apical electrode. Consequently, an individualized frequency map, dependent upon canal length, was computed for each patient.

Given the second assumption, the value for A was calculated based on $F = 20$ Hz at the apical end of the cochlear canal, where $x = 0$ mm and $k = 0.88$ using the formula $A = F/(10^{ax} - k)$; $A = 166.67$. This value of A was then used in Greenwood's formula to calculate a patient-specific value of a using the formula $a_s = \log[(F + kA)/A]/x_s$, where $k = 0.88$, F = 20,000 Hz, and x_s= total length of the individual's cochlear canal in mm (x_s is the same as L_s). These calculations lock the frequency range from 20 to 20,000 Hz. The estimated characteristic frequency (Hz) at the most apical electrode for each patient was calculated with Greenwood's formula using $A = 166.67$, the patient-specific values of a_s, x equals the patient-specific value of cochlear canal length (mm) from the apex to the most apical electrode, and $k = 0.88$.

Word recognition evaluation

Word recognition was evaluated with Cochlear Corporation recordings of monosyllabic words at 3, 6, 8, 12 months after implantation and at yearly intervals thereafter as part of a longitudinal research study started in 1987. The NU-6 word test (Tillman and Carhart 1966) recorded by a male talker of General American dialect was used. Scores reported in the present study are based on the mean of two 50-word lists presented at 70 dB SPL in a double-walled sound booth with the patients sitting at 0° azimuth in front of the loudspeaker. Although 70 dB SPL represents a raised-to-loud vocal effort, word recognition testing for patients in the longitudinal study began before it was verified that those using the SPEAK strategy could recognize a substantial number of words and sentences at a normal vocal effort of 60 dB SPL (Skinner et al. 1997). To compare speech recognition within and across speech-coding strategies in the same patients over time, it was important to continue testing at 70 dB SPL. Speech processor programs and sensitivity control settings were those that patients used in their everyday lives. They wrote their responses.

For data analysis, linear regression between the word recognition score (obtained after one year of SPEAK use) and array insertion depth was used. Because the number of uncontrolled variables and the variance for each variable were large, the sample size was too small to conduct a meaningful cluster analysis.

RESULTS

Three-dimensional cochlear canal length

Table 4 shows the measured axial heights, basal and middle turn diameters, and hook lengths determined from CT scans for P1 through P13. These patients had cochleae with 2.5 turns, except P10 whose cochlea had 2.75 turns. Also shown in Table 4 are calculated values of the axial turn diameter, spiral constant a, cochlear canal length from apex to the end of the first turn (without the hook), and total cochlear canal length including the hook. These same data are shown for P14 through P26 in Table 3 in Ketten et al. (1998). The mean total cochlear canal length for P1 through 13 was 34.62 mm; the range of individual lengths was 32.94–36.57 mm. The mean cochlear length for males (34.66 mm) was not significantly different from that of females (34.58 mm) in this subpopulation.

Observations of implanted array position in cochlear canal

Visual observations of the implanted array position in the cochlear canal from the series of high-resolution 2D images are summarized in Table 5 for P1 through P13. P10 was the only patient for whom the entry point of the array was near the oval window into scala vestibuli. This entry was made when the surgeon could not find a patent scala tympani in the lower basal turn during surgery. For the other patients, the

TABLE 4

Cochlear measurements

	Cochlear canal measurements (mm)				*Calculated values*			
							Cochlear length (mm)	
Patient	*Axial Height*	*Basal* diameter	*Middle diameter*	*Hook*	*Apical diameter (mm)*	*Spiral constant*	*Without hook*	*With hook*
1	2.58	8.39	4.84	2.59	1.29	0.27	33.56	36.15
2	2.19	8.34	4.94	2.58	1.88	0.27	33.36	35.94
3	1.88	7.80	4.69	2.53	1.56	0.25	31.18	33.71
4	2.31	8.10	5.00	2.56	1.88	0.26	32.40	34.96
5	2.50	7.80	3.75	2.53	1.56	0.25	31.22	33.75
6	1.88	8.50	4.69	2.60	1.56	0.27	33.97	36.57
7	2.50	8.30	3.75	2.58	1.56	0.26	33.21	35.79
8	2.81	7.70	4.69	2.52	1.56	0.25	30.85	33.37
9	2.50	7.60	4.69	2.51	1.56	0.24	30.43	32.94
10	2.81	7.90	5.00	2.54	1.88	0.25	31.65	34.19
11	2.03	7.66	4.38	2.52	1.25	0.24	30.62	33.14
12	2.50	8.10	4.38	2.56	1.25	0.26	32.41	34.97
13	2.30	8.00	4.50	2.55	1.50	0.26	32.00	34.55
Mean	2.37	8.01	4.56	2.55	1.56	0.26	32.07	34.62
SD	0.31	0.30	0.41	0.03	0.22	0.01	1.19	1.22
Minimum	1.88	7.60	3.75	2.51	1.25	0.24	30.43	32.94
Maximum	2.81	8.50	5.00	2.60	1.88	0.27	33.97	36.57
Median	2.50	8.00	4.69	2.55	1.56	0.26	32.00	34.55

array entered the lower basal turn with considerable variability in angle of insertion. At the entry, the arrays for P5, P6, P12, and P13 appeared to cross from scala vestibuli (SV) to scala tympani (ST), whereas for the others they went into scala tympani. For P3, P4, P9, and P13, there are scala vestibuli to scala tympani excursions of the array in the lower/middle basal turn. A number of patients had kinks in the array within the cochlea, particularly P4 and P7, and some had compressions or twists in the array. Observations of the electrode array trajectory in the cochlear canal are given for P14 through P26 in Table 5 of Ketten et al. (1998); for these patients, the array was implanted in the scala tympani.

Three-dimensional electrode array reconstructions for six patients were chosen to illustrate the electrode array trajectory (Fig. 2). For each patient, different 3D orientations of the array were chosen to optimize visualization of the idiosyncrasies of the array paths. The arrows in Figure 2 point to the entry point of the arrays into the cochlea. For P12 and P7, the array images terminate in the middle ear very close to the array paths' entry into the cochlea. For P3, P4, P5, and P10, the array image has been truncated in the middle ear at different distances from cochlear entry. P12's array has a circular configuration with insertion of all electrodes and supporting bands into the cochlea; kinking at the ascent into the upper basal turn and again at the ascent into the second turn are evident. There is a shallow insertion of P10's array into the cochlea with compression as it ascends apically with the tip electrode shown at the far right of the image. The compression is probably related to the array's insertion into the scala vestibuli (SV) near the oval window and the tip electrode jamming against the outer bony wall. P5's array has a sharp U-shaped kink just before its entry into the cochlea and a curved trajectory across scalae in the lower to middle basal turn. P7's array has a sharp kink just after its entry into the cochlea. For this patient, the surgeon's records indicate it was necessary to drill through otosclerotic bone to reach fluid and presumably a patent scala tympani (ST). This drilled region is consistent with the straight trajectory after the kink. The complex 3D trajectory in the middle to upper basal turn resulted from the array confronting a cochlear canal that was severely deformed by otosclerotic changes. P4's array has a complicated 3D trajectory in the basal turn of the cochlea showing repeat SV–ST–SV–ST excursions that may be related to his temporal bone fracture caused by a motorcycle accident.

CT-based estimates of insertion depth of electrode array

Table 6 shows the 3D functional insertion depth of the array for P1 through P13 expressed in mm,

TABLE 5

Qualitative assessment of electrode paths in cochlea–array interactions

Patient	*Entry*	*Lower basal to mid basal turn*	*Upper basal turn to array tip*
1	Drillout evident.	Array at outer bony wall.	Array centered in cochlear canal.
2	Entry near promontory superior to round window. Array enters ST a few mm into basal turn and follows hook curvature. Compression at entry.	Array initially against outer bony wall; impacts outer bony wall after first major bend.	Array impacts outer bony wall in upper basal turn. Tip twisted and bent.
3	Fairly straight entry. Clean cochleostomy.	Array goes diagonally across scala and into ST for ascent into upper basal turn.	Slight kink in array in transverse segment near tip.
4	No drillout; surgeon opened window.	Heavy kinking and extra curving with many SV/ST excursions in lower basal turn. Also modiolar to lateral wall twists.	Array goes into ST during ascent; slight kink in transverse segment.
5	Small kink or crimp at entry.		
6	Relatively straight entry.	Narrow curvature of electrodes 11 and 12.	Compression of electrodes 14–18.
7	Entry into SV with big kink and excursion to ST immediately after insertion.	Array badly twisted and compromised in basal turn near hook.	
8		Basal twists.	
9	Low level, straight in entry.	Moderate SV/ST curve. Indents are compressions of electrode bands.	Tip twisted.
10	Entry just past oval window squared edge cochleostomy.	Curve in array compacted on ascending arm. Dip downward in basal turn. Bone in basal turn.	Tip jammed into wall on ascending arm.
11	Array exceptionally straight with small compression near cochleostomy.	Kinks.	
12	Drill out from scala media or SV to ST.	Kink.	Kink in middle turn.
13	Array entered at promontory and quickly crosses SV into ST.	Obvious SV to ST excursion in basal turn.	Array probably compressed because canal is largely blocked past array.

[a]ST = scala tympani; SV = scala vestibuli.

percentage of total cochlear canal length, and degrees rotation from the apex and from the beginning of the first turn (i.e., not including the hook region). The mean insertion depth in mm was 18.86 mm and the range of individual values was 11.87–25.93 mm. The distribution of the ranges between male and female patients did differ (11.87–21.71 mm for males; 11. 98–25.93 mm for females). However, there was little difference in mean insertion depth in mm between male and female patients (18.61 vs. 19.07 mm, respectively) or in mean percentage of cochlear canal length covered by the array (54% for males and 55% for females). For P1 through P13, the mean insertion depth in degrees rotation from the apex was 575° and 330° from the beginning of the first cochlear turn. Table 3 in Ketten et al. (1998) gives the 3D functional insertion depth of the array expressed in mm and in percentage of total cochlear length for P14 through P26.

Estimates of insertion depth of electrode array from surgeon's observations

Figure 3 shows the estimates of insertion depth (mm) from the surgeon's report and the manufacturer's specifications for electrode array distances plotted as a function of the CT-derived estimates for all 26 patients. The mean insertion depth estimated from the surgeon's report and the manufacturer's specifications was 20.83 mm; this depth is 1.14 mm longer than that estimated from the CT data. The fact that the CT-derived mean insertion depth is shorter than the surgeon's report is consistent with the observations of compressions and kinks in the array that the surgeon could not see after insertion. Linear regression of the CT-derived insertion depth of the array in mm as the dependent variable showed significant correlation with the insertion depth of the array in mm estimated from the surgeons' report ($R = 0.81$,

TABLE 6

CT-based estimates of array insertion depth

Patient	Total cochlear length (mm)	Functional array insertion length (mm)	Array insertion length/ cochlear length	Apical electrode position from apex (degrees)	Apical electrode position from beginning of first turn (degrees)
1	36.15	19.18	0.53	585	315
2	35.94	19.52	0.54	575	325
3	33.71	17.67	0.52	588	312
4	34.96	21.26	0.61	522	378
5	33.75	19.10	0.57	556	344
6	36.57	22.36	0.61	520	380
7	35.79	21.71	0.61	524	384
8	33.37	19.05	0.57	552	344
9	32.94	16.95	0.51	595	287
10	34.19	11.87	0.35	800	190
11	33.14	18.55	0.56	560	333
12	34.97	25.93	0.74	394	507
13	34.55	11.98	0.35	710	190
Mean[a]	34.62	18.86	0.54	575	330
SD	1.22	3.85	0.10	97	82
Minimum	32.94	11.87	0.35	394	190
Maximum	36.57	25.93	0.74	800	507
Median	34.55	19.10	0.56	560	333

[a]Arithmetic means.

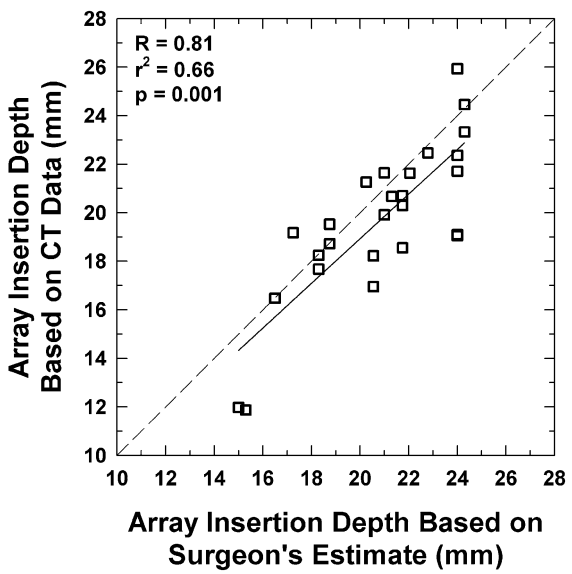

FIG. 3. Electrode array insertion depth in mm estimated from CT analysis and from the surgeon's report and nominal measurements of the array dimensions for the 26 patients. The dashed line represents the points at which the insertion depths would be the same as estimated from CT analysis and the surgeon's report. The linear regression line, correlation, and significance values are shown.

$r^2 = 0.66$, $p = 0.001$). The fact that the regression line lies below the equality line (dashed line in Fig. 3) shows that, on average, array insertion depth estimated from the surgeon's report is longer than the CT-derived estimate. Although there is a strong linear relation between these two estimates of array insertion depth, there were a number of patients for which there was a relatively large difference in the insertion depth estimates. For example, insertion depth reported by the surgeon for P5 and P7 was 4.95 and 4.90 mm longer than that based on CT analysis, respectively. In contrast, CT-derived insertion depth was 1.93 mm longer than that reported by the surgeon for P1 and P12.

Estimates of cochlear and array characteristic frequency distributions

Characteristic frequencies at the apical and basal ends of the cochlear canal (including the hook), as well as those at the most apical electrode in the array, were calculated based on the following assumption: The total range of hearing (Hz) differs for different cochleae because each critical band covers the same linear distance along the basilar membrane (i.e., variable hearing range). These values are given for P1 through P13 in Table 7 and for P14 through P26 in Table 3 in Ketten et al. (1998). For P1 through P13, the calculated harmonic mean characteristic frequency was 20 Hz at the apical end of the cochlea and 21,113 Hz at the basal end using Greenwood's basic formula with a constant of 165.4. This result compares reasonably well with the generally accepted fixed hearing range of 20–20,000 Hz; however, the calculated mean characteristic fre-

TABLE 7

Calculated characteristic frequencies for each patient using different Criteria

Patient	*Frequency at apex (Hz) re 35-mm-long cochlea*	*Frequency at basal end of Cochlea (Hz) re 35-mm-long cochlea*	*Frequency at apical electrode (Hz) re 35-mm-long cochlea*	*Frequency at apical electrode (Hz) for frequency range 20–20,000 Hz*
1	19	19,380	1365	1436
2	19	19,608	1290	1343
3	21	22,294	1624	1485
4	20	20,724	957	944
5	21	22,236	294	1189
6	18	18,945	858	927
7	19	19,775	921	953
8	22	22,746	1289	1158
9	22	23,350	1787	1562
10	21	21,675	3919	3666
11	22	23,071	1388	1229
12	20	20,708	433	429
13	20	21,218	3848	3674
Mean[a]	20	21,113	1174	1147
SD	1.43	1484	1066	992
Minimum	18	18,945	433	429
Maximum	22	23,350	3919	3647
Median	20	21,218	1294	1229

[a]Harmonic means.

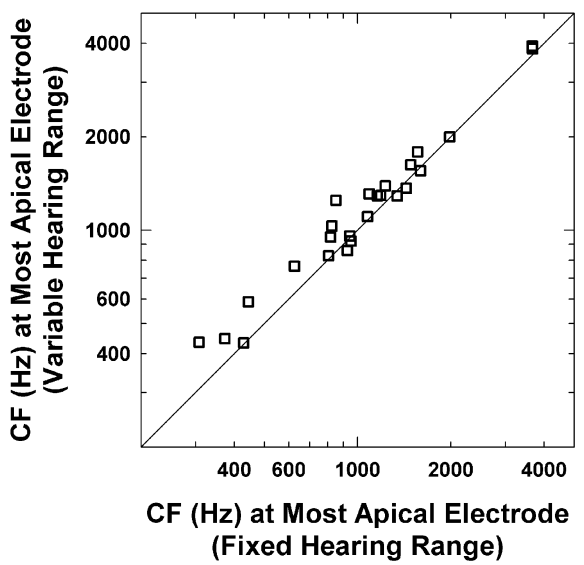

FIG. 4. Characteristic frequency (CF) in Hz at the most apical electrode calculated for the variable and fixed hearing ranges for the 26 patients. The diagonal line represents the points at which the characteristic frequencies calculated for the variable and fixed hearing ranges would be the same for an individual patient.

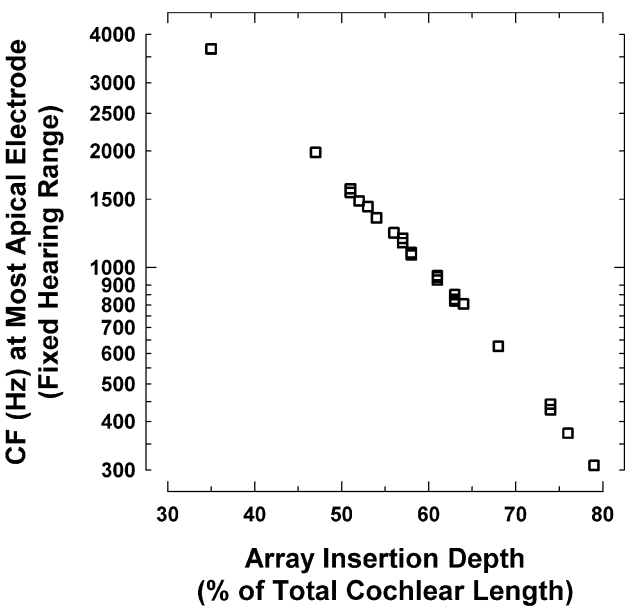

FIG. 5. Characteristic frequency (CF) in Hz at the most apical electrode calculated based on the fixed frequency range of 20–20,000 Hz as a function of array insertion depth as a percentage of total cochlear length.

quency at the basal end of the cochlea for individuals with short cochlear canals (P9 and P11) was substantially higher than 20,000 Hz (23,350 and 23,071 Hz). For all 26 patients, the range of characteristic frequencies associated with the most apical electrode was large (4334–3919 Hz) for a variable hearing range using 35-mm normalized data as well as the data locked to a fixed 20–20-kHz range (429–3674) across cochlear lengths. These data are plotted in Figure 4. If the characteristic frequencies were identical for the variable and fixed hearing ranges, the points would lie along the diagonal. Although the values lie close to the diagonal, the range of

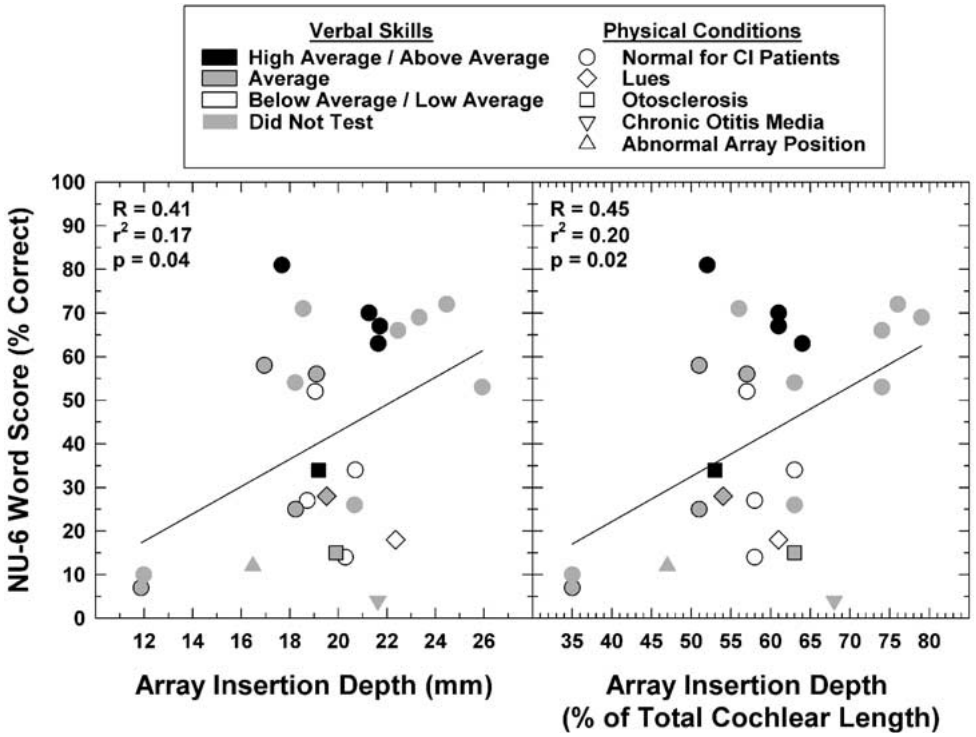

FIG. 6. Electrode array insertion depth in mm (left panel) and percentage total cochlear length (right panel) for the 26 patients. The linear regression line, correlation, and significance values are shown in each panel. Symbol shapes denote physical status of the cochlea and position of electrode array (see text for description). Black, gray, and white shading of symbols encircled in black denotes three ranges of verbal IQ scores (Wechsler 1981) for the 16 patients tested. Gray shading with encircling in gray is used for the 10 patients whose verbal IQ scores were not obtained.

differences in characteristic frequency varies from 4 Hz for P12 to 253 Hz for P10.

Relation of array insertion depth to characteristic frequency at most apical electrode

Figure 5 shows the estimated characteristic frequency assuming a normal acoustic tonotopic pattern as a function of insertion depth at the most apical electrode for the 26 patients. These characteristic frequencies were calculated for the fixed frequency range between 20 and 20,000 Hz using the patient-specific constant a_s, that takes into account the total length of that individual's cochlear canal instead of assuming an average 35-mm-long cochlea. Array insertion depth has been expressed in percentage of total cochlear length to account for the large variation in total cochlear canal length among these patients (29.07–36.15 mm). The estimated characteristic frequencies associated with the shallowest insertion depth (35% for P11 and P13) are 3666 and 3674 Hz, respectively, and that for the longest insertion depth (74% for P22) is 308 Hz.

Patients 8 and 13 used the Common Ground mode with the most apical electrode in the array (electrode 22) as an active electrode, whereas three other patients (P10, P17, and P21) who used the Common Ground mode did not use electrode 22 (see Table 3). The other patients used a bipolar mode for which electrode 22 was the return electrode. For these patients, it is unknown whether the highest density of electrical current is halfway between the active and return electrodes or at some other location. Because of this uncertainty and the fact that the location of electrodes other than electrode 22 cannot be determined based on the spiral CT scan data obtained for this study, a direct comparison between the frequency band assigned to the most apical electrode in a patient's speech processor program (as shown in Table 3) and the characteristic frequency estimated at the position of electrode 22 was not made.

Relation of word recognition and insertion depth

The NU-6 word score for the 26 patients after one year of SPEAK use is shown in Table 2. These scores are plotted as a function of array insertion depth in mm (Figure 6, left panel) and in percentage of total cochlear length (Fig. 6, right panel) based on analysis of images reconstructed from the CT data. Each patient's symbol denotes aspects of the physical condition of the cochlea (or position of the electrode array in the cochlea) and his/her verbal skills. The 10 patients whose verbal skills were not evaluated have symbols that are not outlined in black, and the 20 patients for whom the physical condition of the cochlea or the electrode position was normal have symbols that are circles. Other symbols are described below. Linear regression, with the word scores as the dependent variable, showed significant correlation with the CT-derived insertion depth of the array in

TABLE 8

Cochlear canal length and array insertion length for patients across both studies

	Total cochlear length (mm)	*Functional array insertion length (mm)*	*Array insertion length/ cochlear length*
Ketten et al. study			
Mean[a]	33.01	20.19	0.61
SD	2.31	2.86	0.09
Minimum	29.07	13.68	0.46
Maximum	37.45	24.46	0.79
Median	32.64	20.69	0.63
Both studies			
Mean[a]	33.64	19.67	0.59
SD	2.09	3.28	0.10
Minimum	29.07	11.87	0.35
Maximum	37.45	25.93	0.79
Median	33.75	19.91	0.58

[a]Arithmetic means.

mm ($R = 0.409$, $r^2 = 0.167$, $p = 0.038$) and the CT-derived insertion depth of the array in percentage of total cochlear length ($R = 0.452$, $r^2 = 0.204$, $p = 0.020$). As shown in the right panel of Figure 6, the two patients with the shallowest array insertion depth (35% of the total cochlear length) had among the lowest scores, and the four patients with the deepest insertions (74%–79% of the total cochlear length) had among the highest scores. For intermediate array insertion depths between 47% and 68% of the total cochlear length (16.47 and 21.63 mm), the word scores ranged from the lowest to the highest (4%–81% correct) in this study. For these 20 patients, the relation between word score and insertion depth is obscured. Below, we present reasonable hypotheses about other factors that contribute to word scores in cochlear implant patients. For example, we will argue that some patients' word scores are lower than normal because the physical condition of the cochlea limits the amount of information transmitted to the central auditory nervous system and/or their verbal skills are below average.

DISCUSSION

Cochlear canal and electrode array insertion lengths

The group mean cochlear canal length and CT-derived functional array insertion length (expressed in mm and as a percentage of the cochlea occupied by the implanted array) for the 20 patients in the Ketten et al. study (1998) are shown in the top half of Table 8. When the data for that group are combined with the data for the 13 patients in the present study, the mean length (33.64 mm) is shorter than the average-length cochlea (35 mm) used by Greenwood (1990) and others who follow his criteria in the calculation of characteristic frequencies. However, this mean length is not significantly different from the majority of temporal bone study data previously reported (e.g., Ulehlova et al. 1987). The range of individual patients' cochlear canal lengths spans more than 8 mm (29.1–37.4 mm). The mean insertion depth was longer in the Ketten et al. study (1998) than across both studies mainly because P10 and P13 in the present study had exceptionally shallow insertions.

As shown in Figure 3, estimates of array insertion depth based on the surgeon's report differ substantially from CT-derived measures for a number of patients. The presence of compressions (P10 and P13) and kinks (P4 and P7), seen in the 3D reconstructed images of the electrode array trajectory in Figure 2 (as well as Figs. 6 and 8 in Ketten et al.), clearly indicate the importance of *in-vivo* radiologic imaging to determine the position of the implanted electrodes. Although schematic representations of the tonotopic location of Nucleus-22 electrodes inserted into the cochlea provide a simplified approximation (e.g., Fig. 1 in Fu and Shannon 1999b), CT-based analysis of the electrode array position provides a closer estimation of its actual position and explicit trajectory in each patient.

Relation between characteristic frequency and frequency band assigned to most apical electrode

For all 26 patients, the lowest frequency of incoming sound was assigned to the most apical electrode in the speech processor program. This electrode was either the return electrode for a bipolar pairing mode or the active electrode for the Common Ground mode of stimulation. With decreasing

insertion depth, there was an increasing mismatch between the characteristic frequency of neurons near the most apical electrode and the frequency band assigned to it (see Fig. 5). For example, the estimated characteristic frequency of neurons near electrode 22 was 1485 Hz for P3 and 1229 Hz for PI 1. Both patients used electrode 22 as the return electrode for electrode 20 to which the frequency band from 120 to 280 Hz was assigned. The shift in frequency was over 1000 Hz at electrode 22. If a position halfway between electrodes 22 and 20 had been chosen as an estimated center of stimulation for biphasic pulses, the frequency shift would have been less but still substantial. For P12, P21, P22, and P24, who had the longest insertion depths, there was a small mismatch. In contrast, for P10 and P13, who had the shallowest insertion depths, the mismatch was over 3300 Hz.

Effect of array insertion depth and other factors on word recognition

There was a modest significant correlation between array insertion depth and word recognition after one year of SPEAK speech-coding use. The significance of this correlation was expected given the increasing mismatch between characteristic frequency of neurons and the frequency bands of incoming sound assigned to the electrodes as the array insertion depth decreases. It also was expected that this correlation would be modest given other factors that affect word recognition. Ideally, the amount of variability contributed by these other factors could be analyzed with multiple regression but the sample size is too small and the range over which other factors vary is large in our sample. Nevertheless, it is important to access the information available in an attempt to gain some understanding for the large spread of word scores for patients with array insertion depths between 47% and 68% of the total cochlear canal length.

A primary factor affecting word recognition (Blamey et al. 1996) is the physical condition of the cochlea. Word scores for patients whose physical status of the cochlea or implanted array's position were that expected for the majority of the world population of implant recipients are shown by circles in Figure 6. Other symbol shapes are used for word scores for six patients for whom these conditions appeared abnormal. Two patients had a luetic infection (diamond symbol) that caused their total deafness as well as severe destruction of sensory and neural cells in the cochlea (Schuknecht 1993). The one with the lowest score (18%) also had central auditory processing and word recall problems that may have been the result of the luetic infection affecting her brain. One patient (P25) had chronic otitis media with presumed bacterial labyrinthitis (inverted triangle symbol) that also caused severe destruction of sensory and neural cells in the cochlea. Two patients had otosclerosis (square symbol) with three or four apical electrodes that cause facial nerve stimulation. Not only did these electrodes have to be eliminated from the speech processor program, but the frequency bands of incoming sound below 1000 Hz that would have been assigned to them had to be assigned to more basal electrodes with greater mismatch between these assigned bands and the characteristic frequencies of nearby neurons. Because the otic capsule lacked the normal insulating properties for electrical stimulation from apical electrodes that remained in their programs, current paths from these electrodes may have been aberrant and caused channel interactions that interfered with speech recognition. Two other patients (P7 and P26) had otosclerosis but apical electrodes did not cause facial nerve stimulation. One patient had an abnormal position of the electrode array (triangle symbol). The array was backfolded just after its entry into the cochlea. On the basal electrodes in this region of backfolding, this patient's thresholds were very low and growth of loudness was very slow. Stimulation on these electrodes may have caused aberrant current paths. The array also was twisted at the position of three more electrodes, one of which had a shorted lead wire and two produced abnormal sound quality. These electrodes were eliminated from the speech processor program. The abnormal position and function of the array appeared to adversely affect the word recognition score.

Verbal ability is a factor related to central neural survival and function, memory for spoken language, and the processes of plasticity and learning. For the 16 patients who were evaluated with the Wechsler Adult Intelligence Scale-Revised (see Table 2), their verbal IQ scores were categorized as high average and above average (117–136), average (87–114), or low average to below average (could not test to 83) as shown by the black, gray, and white shading encircled in black, respectively, in Figure 6. The 10 patients who were not tested are represented by the gray shading with no black encircling. Four patients with partial array insertion (52%–61% of total cochlear length) and word scores between 63% and 81% correct had high-average or above-average verbal IQ scores and they ranged in age from 30 to 74 years when tested. These word scores were well above the regression line and the group mean of 41.8%. Four more patients with partial array insertion (58%–63% of total cochlear length) and word scores between 18% and 34% correct had below-average or low-average verbal IQ scores. They ranged in age from 38 to 78 years when tested. Their word scores were well below the regression line. Of

these four, P6 and P15 had etiologies associated with central auditory processing difficulties, and P19 was in the early stages of Alzheimer's disease. In contrast, one patient (P8) with a below-average verbal IQ score and a partial array insertion had a word score of 52%, which was above the regression line. Her below-average verbal IQ score may have reflected the fact that she did not use a hearing aid until grade school and had no special training to compensate for her hearing impairment.

Of the 26 patients, only P10, P19, and P26 showed no improvement in word score over a number of years of SPEAK use. Although P10 had a shallow insertion, his lack of improvement probably is related to not using his implant at work due to the high noise levels. In addition, he does not always use his implant at home because he can still communicate with relative ease given his exceptional lipreading abilities and average verbal IQ. Consequently, he has had much less experience listening with his implant than other patients in this study who all used their implant processors for 12–18 hours a day. P19 and P26 both had decrements in word score from that obtained after one year of implant use. P19 stopped using her speech processor after four years of SPEAK use because of advanced Alzheimer's disease, and P26 died after two years of SPEAK use. For the other 23 patients, average word score improvement was 12.6 percentage points during the years of SPEAK use and ranged from 6 to 27 percentage points for individual patients. These results and patients' self-reports provide evidence that they learned to recognize words substantially better after four months to seven years of SPEAK use. It appears that those patients for whom there was a mismatch between the estimated characteristic frequency of neurons near each stimulating electrode and the frequency band of sound assigned to it accommodated at least partially to this mismatch. This result is in agreement with that of Fu and Shannon (1999a,b,c) whose subjects accommodated atleast partially to the frequency allocation in the speech processor programs they had been using in everyday life. They also found that the frequency allocation associated with peak performance on vowels was similar for individuals whose electrode insertion depth differed by 7 mm. Among the 26 patients in the present study, P3 has the highest word score of 81% with a partial array insertion depth of 17.67 mm, and P24 has a word score of 72% with a complete insertion depth of 24.46 mm, a difference of 6.79 mm. This result agrees closely with that of Fu and Shannon (1999c). In the present study, the point of incomplete accommodation appears to be for an array insertion depth between 35% and 52% of the total cochlear length based on the word scores of 10% and 81% correct for P13 and P3, respectively.

SUMMARY AND CONCLUSIONS

The significant correlation of word scores with insertion depth of a cochlear implant array for the 26 Nucleus-22 recipients who used the SPEAK strategy for one year suggests that part of the variability in speech recognition can be accounted for by the position of the electrode array in the inner ear. Comparison of an individual patient's word recognition score with etiology of deafness, electrodes that caused facial nerve stimulation (for P1 and P17 with otosclerosis), evidence of central auditory processing difficulty (P6 and P19), lack of sufficient implant use for consistent learning (P10), and verbal IQ scores that ranged from below to above average provided insights into factors other than array insertion depth that affect these scores. The improvement in word scores during use of the SPEAK strategy by all but a few patients lent support for the hypothesis that most of the patients accommodated at least in part to the shift in frequency of incoming sound to a higher pitch percept with the implant than would normally be perceived acoustically.

The higher correlation value for insertion depth expressed as a function of percentage of total cochlear length compared with insertion depth in mm suggests that determination of an individual's cochlear length is important. Although there is a significant correlation between array insertion depth (mm) from CT-derived estimates and estimates from the surgeon's report and manufacturer's specifications of array length, the insertion depth was 1.16 mm shorter based on CT measures. More important, insertion depth based on the surgeon's report ranged from 1.93 mm shorter to 4.95 mm longer for individual patients. Given these large differences, CT-based analysis of the electrode array position appears to provide a closer estimation of its actual position and trajectory in the cochlea than the approximation based on the surgeon's report.

This study's sample size was small and other factors that affect word recognition varied widely. Further study with a larger sample size and direct assessment of other factors (e.g., working memory, learning as it affects word recognition during the first two years of implant use) is warranted.

ACKNOWLEDGMENTS

We are grateful to the cochlear implant patients who participated in this study as well as to Roberta L. Yoffie, RT(R), and Patricia M. Suntrup, RT(R), who coordinated their radiological evaluations. We are also grateful to Elizabeth J. Neetles, Ph.D., who obtained the Wechsler verbal IQ measures as part of her preoperative psychological evaluation of these patients. We are indebted to Siemens and Willi Kal-

endar, Ph.D., for use of the submillimeter and scale expansion software that was a valuable tool for reconstruction of Somatom PLUS S spiral CT data. Timothy Holden, Scott Cramer, Bruce Whiting, Ph.D., and Franz J. Wippold, M.D., provided helpful critiques and assistance with the preparation of this manuscript. Research was supported by a grant from the National Institute on Deafness and Other Communication Disorders (DC00581) as well as assistance from Siemens Medical Systems, Inc., the Electronic Radiology Laboratory at Washington University School of Medicine, and the Department of Radiology, Massachusetts Eye and Ear Infirmary, Boston, Massachusetts. We are grateful to Dr. Richard Robb of the Mayo Clinic for access to the ANALYZE™ software.

REFERENCES

BLAMEY P, ARNDT P, BERGERON F, BREDBERG G, BRIMACOMBE J, FACER G, LARKY J, LINDSTRÖM, NEDZELSKI J, PETERSON A, SHIPP D, STALLER S, WHITFORD L. Factors affecting auditory performance of postlinguistically deaf adults using cochlear implants. Audiol. Neurootol. 1:293–306, 1996.

BREDBERG G. Cellular pattern and nerve supply of human organ of Corti. Acta Otolaryngol. (Stockh) Suppl. 236:1–135, 1968.

BUUS S, FLORENTINE, M, MASON CR. Tuning curves at high frequencies and their relation to the absolute threshold curve. In: Moore BCJ, Patterson RD (eds) Auditory frequency selectivity. J. New York, Plenum, pp 341–350, 1986.

COHEN LT, BUSBY PA, CLARK GM. Cochlear implant place psychophysics. 2. Comparison of forward masking and pitch estimation data. Audiol. Neurootol. 1:278–292, (1996a).

COHEN LT, XU J, XU SA, CLARK GM. Improved and simplified methods for specifying positions of the electrode bands of a cochlear implant array. Am. J. Otol. 17:859–865, (1996b).

DOWELL RC, SELIGMAN PM, BLAMEY PJ, CLARK GM. Speech perception using a two-formant 22-electrode cochlear prosthesis in quiet and in noise. Acta Otolaryngol. 104:439–446, 1987.

FU Q-J, SHANNON RV. Effects of electrode location and spacing on phoneme recognition with the Nucleus-22 cochlear implant. Ear Hear. 20:321–331, (1999a).

FU Q-J, SHANNON RV. Recognition of spectrally degraded and frequency-shifted vowels in acoustic and electric hearing. J. Acoust. Soc. Am. l05:1889–1900, (1999b).

FU Q-J, SHANNON RV. Effects of electrode configuration and frequency allocation on vowel recognition with the Nucleus-22 cochlear implant. Ear Hear. 20:332–344, (1999c).

GREENWOOD DD. Critical bandwidth and the frequency coordinates of the basilar membrane. J. Acoust. Soc. Am. 33:1344–1356, 1961.

GREENWOOD DD. A cochlear frequency–position function of several species—29 years later. J. Acoust. Soc. Am. 87:2592–2605, 1990.

GREENWOOD DD, JORIS PX. Mechanical and ''temporal'' filtering as codeterminants of the response by cat primary fibers to amplitude-modulated signals. J. Acoust. Soc. Am. 99:1029–1039, 1996.

HELMS J, MULLER J, SCHON F, MOSER L, ARNOLD W, JANSSEN T, RAMSDEN R, VON ILBERG C, KIEFER J, PFENNINGDORF T, GSTOTTNER W, BAUMGARTER W, EHRENBERGER K, SKARZYNSKI H, RIBARI O, THUMFART W, STEPHAN K, MANN W, HEINEMANN M, ZOROWKA P, LIPPERT KL, ZENNER HP, BOHNDORF M, HUTTENBRINK K, MULLER–ASCOFF E. Evaluation of performance with the COMBI40 cochlear implant in adults: A multicentric clinical study. ORL J. Otorhinolaryngol. Relat. Spec. 59:23–35, 1997.

KELSALL DC, SHALLOP JK, BRAMMEIER TG, PRENGER EC. Facial nerve stimulation after Nucleus 22-channel cochlear implantation. Am. J. Otol. 18:336–341, 1997.

KETTEN DR. The role of temporal bone imaging in cochlear implants. Curr. Opin. Otolaryngol. Head Neck Surg. 2:401–408, 1994.

KETTEN DR, SKINNER MW, WANG G, VANNIER MW, GATES GA, NEELY JG. In vivo measures of cochlear length and insertion depth of nucleus cochlear implant electrode arrays. Ann. Otol. Rhinol. Laryngol. (Suppl. 175) 107:1–16, 1998.

KETTEN DR, WARTZOK D. Three-dimensional reconstructions of the dolphin ear. In: Thomas J, Kastelein R (eds) Sensory abilities of cetaceans. New York, Plenum Press, pp 81–105, 1990.

MARSH MA, XU J, BLAMEY PJ, WHITFORD LA, XU SA, SILVERMAN JM, CLARK GM. Radiologic evaluation of multichannel intracochlear implant insertion depth. Am. J. Otol. 14:386–391, 1993.

MOORE, BCJ, GLASBERG BR, BAER T. A model for the prediction of thresholds, loudness, and partial loudness. J. Audio Eng. Soc. 45:224–240, 1997.

NADOL JB Jr, SHIAO JY, BURGESS B, KETTEN DR, EDDINGTON DK, GANTZ BJ, KOSS I, MONTANDON P, COKER NJ, ROLAND JT Jr, SHALLOP JK. Histopathology of cochlear implants. Ann. Otol. Rhinol Laryngol. 110:883–891, 2001.

OSBERGER MJ, FISHER LJ. SAS–CIS preference study in postlingually deafened adults implanted with the Clarion cochlear implant. Ann. Otol. Rhinol. Laryngol. (Suppl. 177) 108:74–79, 1999.

OU HC, HARDING GW, BOHNE BA. An anatomically based frequency-place map for the mouse cochlea. Hear. Res. 145:123–129, 2000.

SCHUKNECHT HF. Pathology of the Ear, 2nd ed. Philadephia, Lee and Febinger, pp 247–253, 1993.

SKINNER MW. Optimization of benefit from a cochlear implant by a multi-disciplinary team. Jpn. J. Logoped. Phoniatr. 40:156–163, 1999.

SKINNER MW, ARNDT PL, STALLER SJ. Nucleus 24 advanced encoder conversion study: performance versus preference. Ear Hear. 23, Suppl. 1: 25–175, 2002.

SKINNER MW, CLARK GM, WHITFORD LA, SELIGMAN PM, STALLER SJ, SHIPP DB, SHALLOP JK, EVERINGHAM C, MENAPACE CM, ARNDT PL, ANTOGENELLI T, BRIMACOMBE JA, PIJL S, DANIELS P, GEORGE CR, MCDERMOTT HJ, BEITER AL. Evaluation of a new spectral peak coding strategy for the Nucleus 22 Channel Cochlear Implant System. Am. J. Otol. 15 (Suppl. 2):15–27, 1994.

SKINNER MW, HOLDEN LK, HOLDEN TA, DOWELL RC, SELIGMAN PM, BRIMACOMBE JA, BEITER AL. Performance of postlinguistically deaf adults with the Wearable Speech Processor (WSPIII) and Mini Speech Processor (MSP) of the Nucleus Multi-Electrode Cochlear Implant. Ear Hear. 12:3–22, 1991.

SKINNER MW, HOLDEN LK, HOLDEN TA, DEMOREST ME, FOURAKIS MS. Speech recognition at simulated soft, conversational, and raised-to-loud vocal efforts by adults with cochlear implants. J. Acoust. Soc. Am. 101:3766–3782, 1997.

TAKAGI A, SANDO I. Computer-aided three-dimensional reconstruction: a method of measuring temporal bone structures including the length of the cochlea. Ann. Otol. Rhinol. Laryngol. 98:515–522, 1989.

TILLMAN TW, CARHART R. (1966) An expanded test for speech discrimination utilizing CNC monosyllabic words: Northwestern University Auditory Test No. 6. Tech. Rep. No. SAM-TR-66-55. USAF School of Aerospace Medicine, Brooks Air Force Base, TX

ULEHLOVA L, VOLDRICH L, JANISCH R. Correlative study of sensory cell density and cochlear length in humans. Hear. Res. 28:149–151, 1987.

WECHSLER D. (1981) Wechsler Adult Intelligence Scale-Revised Manual. New York, the Psychological Corporation.

XU J, XU S-A, COHEN LT, CLARK GM. Cochlear view: post-operative radiography for cochlear implantation. Am. J. Otol. 21:49–56, 2000.

ZHOU B. Auditory filter shapes at high frequencies. J. Acoust. Soc. Am. 98:1935–1942, 1995.